IEEE Access
Multidisciplinary | Rapid Review | Open Access Journal

Received 22 May 2025, accepted 7 June 2025, date of publication 12 June 2025, date of current version 19 June 2025.

Digital Object Identifier 10.1109/ACCESS.2025.3579079

APPLIED RESEARCH

CAD of Antenna Feed Systems With Tracking Capabilities by Controlling High Order Modes

JUAN LUIS CANO[1], GABRIELE CECCATO[2,3], (Member, IEEE), AND LUCA PERREGRINI[3], (Fellow, IEEE)

[1]Department of Communications Engineering, Universidad de Cantabria, 39005 Santander, Spain
[2]Department of Electronic and System Engineering, RINA Consulting S.p.A., 16128 Genoa, Italy
[3]Department of Electrical, Computer, and Biomedical Engineering, University of Pavia, 27100 Pavia, Italy

Corresponding author: Juan Luis Cano (juanluis.cano@unican.es)

This work was supported in part by Consejería de Industria, Empleo, Innovación y Comercio, Gobierno de Cantabria, Spain, under Grant 2023/TCN/005; and in part by Fondo Europeo de Desarrollo Regional (FEDER) Funds [European Union (EU)], for Cantabria under Program FEDER 2021-2027.

ABSTRACT This work presents a workflow to simplify the design process, simulation effort and verification scheme, to generate a signal with desired power, polarization and controlled higher-order modes required for aeronautical tracking systems. This workflow is especially suitable for the simulation and analysis of complex antenna feed systems with multimode monopulse tracking capabilities through the emulation of real operation. The presented scheme is based on S-parameters obtained from literature or full-wave simulations and linear techniques, transforming a CAD-FEM problem into a circuital one, that can be easily implemented analytically and processed in commercial schematic simulation tools. The proposed approach is applied to the analysis of an antenna feed system with a resonant TE_{21} tracking coupler, commonly used in tracking systems today and can be easily adapted and/or extended to more complex feed systems working with different tracking couplers and/or high-order modes. Different polarizations and feed settings are analyzed, obtaining useful information on the operation and best configuration of these complex systems.

INDEX TERMS Antenna feed, higher-order modes, monopulse, multimode, simulation, tracking, waveguide.

I. INTRODUCTION

Antenna feed systems designed in waveguide technology are particularly suited for tracking applications due to their minimum losses and high-power handling characteristics. With these characteristics, tracking capability are generally achieved through circuits that enable antennas to follow a target on the move such as a satellite, a military target or an astronomical body. Many different tracking techniques are available on the market and can be classified in four main groups: manual or programmed tracking, monopulse or simultaneous sensing, sequential amplitude sensing and electronic beam squinting [1]. Among these techniques, monopulse is the one mostly used in space and defense applications. Its functionality requires the generation of signals to pilot servo-motors in order to move the antenna toward the target (elevation and azimuth estimates) from a single pulse of information, which provides advantages that make this technique the main trend in present applications [2]. In monopulse systems, data information is typically carried in the fundamental mode, which presents maximum gain in the boresight direction, the so-called SUM signal. Azimuth and elevation signals are extracted from high order modes (HOMs), generated when the target is not aligned, and therefore centered, to the boresight of the antenna, giving rise to the so-called DELTA signal. Consequently, the tracking signals are zero when the target is aligned to the antenna boresight, while different from zero in other cases. HOMs extraction in the waveguide network is the most used strategy within the monopulse technique, resulting in compact and precise tracking systems.

Non-idealities in the generation of SUM and DELTA signals may affect tracking capability, affecting communication and entire system performance. This problem is known

The associate editor coordinating the review of this manuscript and approving it for publication was Shah Nawaz Burokur.

as de-pointing. In modern HOMs monopulse system, the most probable source of problems, and also the key component for the entire system, is the tracking coupler, a circuit designed to separate HOMs that define the SUM and DELTA signals. The tracking coupler based on waveguide technology is usually designed through circular waveguides, sized to manage HOMs such as TM_{01} [3], [4], TE_{21} [5], [6] and/or TE_{01} [7], [8]. It is a complex structure whose design often requires the use of time-consuming electromagnetic (EM) simulation tools working with multimode input signals leading to very tedious process during the optimization stage.

From simulation analysis, the physical behavior of a tracking coupler (as per any other waveguide component) is described through S-parameters, obtaining information regarding ports reflection, transmission losses and port-to-port isolations. The analysis of a complete monopulse tracking system should emulate a realistic input signal in the waveguide network that would be obtained only by modelling the complete monopulse tracking network, the target and their physical distance. Hence, to simulate the tracking coupler and all its waveguide network using an EM source with a desired polarization and to move the source in different directions, retrieving the complete azimuth and elevation response [9].

These analyses are generally carried out through full-wave finite element method (FEM) simulations based on the actual 3D geometry of the circuit (CAD). From these full-wave simulations, S-parameters at the different ports could be analyzed by retrieving the azimuth and elevation signals of the hypothetical target as it moves in space.

Since the monopulse system as well as the target should be included in the analysis, as well as the volume in terms of free space that separates them, the computational costs extent to high levels because the model complexity also depends on the accuracy that the designer need. Finally, all the simulation results need to be post-processed to obtain meaningful results.

In this work, a simple circuital scheme (shown in Fig. 1) to emulate such scenario is proposed, extending the discussion already presented in [10] and [11] through an in-lab HOMs generator, emulating the actual behavior of a real target. The HOMs generator dynamics, analyzed through a commercial FEM simulator (such as HFSS from Ansys or CST Studio Suite from 3DS), can be imported as a text file in terms of S-parameters though a circuital schematic available in most of FEM EM simulators. These parameters have been already successfully obtained to provide a realistic and controlled HOMs generation with known amplitude and phase parameters [10], [11], [12]. The process of gathering all the responses of the waveguide circuit from the desired source positions is not time consuming, due to the circuit simplicity with respect to a FEM analysis, and the computational time of a tracking coupler or even of a complete antenna feed system is reduced to a great extent. To demonstrate its benefit over other FEM techniques, this paper propose a workflow applied to an antenna feed system using a TE_{21} tracking coupler for different polarizations. From this analysis, useful recommendations for tracking receiver designers are presented.

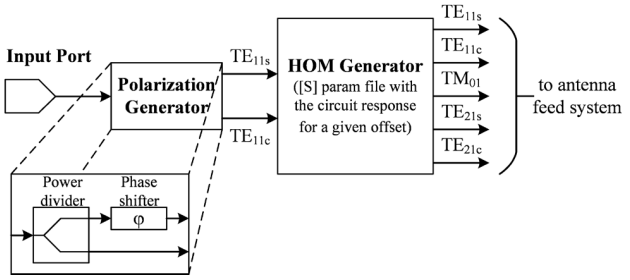

FIGURE 1. Scheme of the proposed circuit for the generation of a signal with known polarization and power, and controlled higher-order modes.

This work is organized as follows: Section II describes the proposed signal generator presented in Fig. 1 and its implementation in a commercial simulation tool such as Microwave Office; Section III introduces and details the antenna feed system that is analyzed afterwards; Section IV presents the computational comparison between different full-wave solvers and the proposed approach; Section V shows results of the analysis performed under different polarizations and tracking receiver configurations, providing useful ideas and recommendations. Finally, Section VI presents all the conclusions that come from this work.

II. SIGNAL SOURCE WITH CONTROLLED HOMS

A. DESCRIPTION OF THE SIGNAL SOURCE

The input signal or generator is presented in Fig. 1. The first element is the Input Port where the desired input power for the fundamental modes, Pin, is defined. Afterwards, a Polarization Generator enables to select between linear, circular or elliptical polarizations by dividing in two the input signal and adding a phase delay term to one of the two branches, to obtain the degenerate fundamental TE_{11} modes. The two branches need to be configured accordingly:

- For linear polarization, both branches must have the same phase shift; therefore, $\phi = 0°$, whereas the power attenuation (ATN) in the power divider follows the relations given by (1) and (2). Each branch corresponds to an axis component of the polarization, so they are called x and y.

$$ATN_x = \frac{P_{in}}{P_x} \tag{1}$$

$$ATN_y = \frac{P_{in}}{P_y} \tag{2}$$

where $P_{x,y}$ are the powers in each branch, that can be calculated from the voltage at the branch, $V_{x,y}$, as

$$P_x = \frac{1}{2}\frac{V_x^2}{Z_0}. \tag{3}$$

$$P_y = \frac{1}{2}\frac{V_y^2}{Z_0}. \tag{4}$$

In (3) and (4) Z_0 is the modal impedance. Finally, the voltages in each branch are related with the total voltage

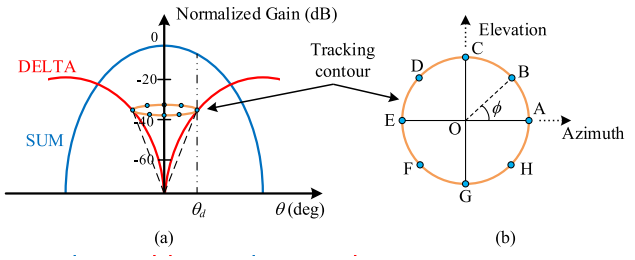

FIGURE 2. (a) Normalized radiation patterns in a typical multimode monopulse system: fundamental mode (blue) and any HOM suitable for tracking purposes (red). (b) For any magnitude of depointing, a circle is obtained (tracking contour), whose circularity can be characterized by a series of discrete points, A to H [10].

at the power divider input, V_i, through the linear polarization angle, α, with respect to the x-axis.

$$V_x = V_i cos(\alpha) \tag{5}$$

$$V_y = V_i sin(\alpha) \tag{6}$$

where,

$$V_i = \frac{1}{2}\sqrt{8Z_0P_{in}}. \tag{7}$$

According to (5), (6), a horizontal linear polarization, aligned with x-axis, is obtained for $\alpha = 0°$; whereas a vertical linear polarization, aligned with y-axis, is achieved with $\alpha = 90°$. Any slant linear polarization can be set by modifying parameter α.

- For circular polarization, both branches need to be in quadrature; therefore, $\phi = \pm 90°$, whereas the power attenuation in each branch is exactly -3 dB. Depending on the sign in ϕ, a left-hand circular polarization (LHCP) or a right-hand circular polarization (RHCP) can be selected.

Once the signal power and polarization are configured, two signals with the corresponding magnitudes and phases, TE_{11}^s and TE_{11}^c, enter the HOMs generator. This is simply a S-parameter file obtained from the literature, full-wave EM simulations or real measurements, containing the response of a circuit where higher-order modes are generated. The generator is a circuit already presented in [10], [11], and [12] where two circular waveguides are not connected aligned along a common axis, but an offset allows the possibility to generate HOMs. According to [11], it can be defined the magnitude of the offset M_0, that is linked to the amplitude of the generated HOMs, while the angle φ allows the excitation of different HOMs. It has been demonstrated that with this circuit it is possible to mimic signals originated from a target in a real application and study the de-pointing effect. Obviously, each pair of values (M_0, φ) produces a S-parameter file therefore, FEM simulation of the waveguide circuit must be repeated in order to have a set of configurations typically used during the calibration of monopulse systems. These files are able to reproduce the tracking contour presented in Fig. 2. Thanks to the simplicity of the circuit presented in [11] and [12] all the aforementioned configurations can be simulated in a short time.

Fig. 2a shows the basic operation performed during the calibration of a typical multimode monopulse system: the antenna is moved along a circular pattern toward a well-known source acting as a target to study possible de-pointing effects. For any de-pointing angle, a tracking contour is obtained (see Fig. 2b). The radius of the circle is related with θ, the angle representing the antenna moving, and therefore is the parameter that characterizes the magnitude of de-pointing. On the other hand, it has been demonstrated in [10] and [11] that it is possible to link the antenna movement with a regular phase φ of the DELTA pattern along the different pointing angles in the range [0, 360°], and therefore the possibility to link the signal phase to the actual antenna pointing angle since the phase of SUM pattern is nearly constant. In this way, making the comparison between phases of SUM and DELTA patterns, the tracking receiver can extract the target position information within the tracking contour obtaining the azimuth and elevation correction signals. To characterize the tracking receiver goodness, it is possible to check the circular symmetry of the tracking contour, by using a series of discrete points, typically eight plus the boresight, as shown in Fig. 2b, requiring a total of nine FEM analysis and therefore nine S-parameters files.

Once retrieved these files, they can be used as input in the circuital scheme presented in this work, giving the advantage to the designer to analyze any kind of tracking circuit with its custom CAD geometry, without the drawback to conduct specific time-consuming FEM analysis on the entire monopulse system. In this way. parameters such as the null depth, the tracking coupling level, the tracking contour symmetry or the tracking-to-information isolation can be easily obtained.

When the input signal exhibits a horizontal polarization (mode TE_{11s} aligned with x-axis) and the waveguide offset with $\varphi = 0°$ and any value of $M_0 \neq 0$, then modes TE_{11s}, TM_{01} and TE_{21s} are obtained at the waveguide output as shown in Fig. 3a. For an offset angle $\varphi = 45°$, modes TE_{11s}, TM_{01}, TE_{21s} and TE_{21c} are present at the output port as presented in Fig. 3b. In this case, power levels of the HOMs are 3 dB below those obtained in the previous case. Finally, with $\varphi = 90°$ only modes TE_{11s} and TE_{21c} are generated. Similar results are obtained for a vertical polarization just exchanging TE_{11s} for TE_{11c} and TE_{21s} for TE_{21c} in Fig. 3. Therefore, mode TM_{01} is not generated when the offset angle is orthogonal to the polarization angle. Consequently, tracking couplers based on mode TM_{01} are not sensitive to elevation or azimuth errors when working with horizontal or vertical polarizations respectively.

For this reason, if linear polarization is used, the tracking receiver needs to manage, at least, two higher-order modes: $TM_{01} + TE_{01}$ [8], [13], $TM_{01} + TE_{21}$ (sine and/or cosine) [14] or TE_{21} (sine and cosine) [15], [16]. On its side, when working with a circular polarization (RHCP or LHCP), all the HOM are generated (TM_{01}, TE_{21s}, TE_{21c}) for any offset angle. Thus, a tracking receiver sensitive to azimuth

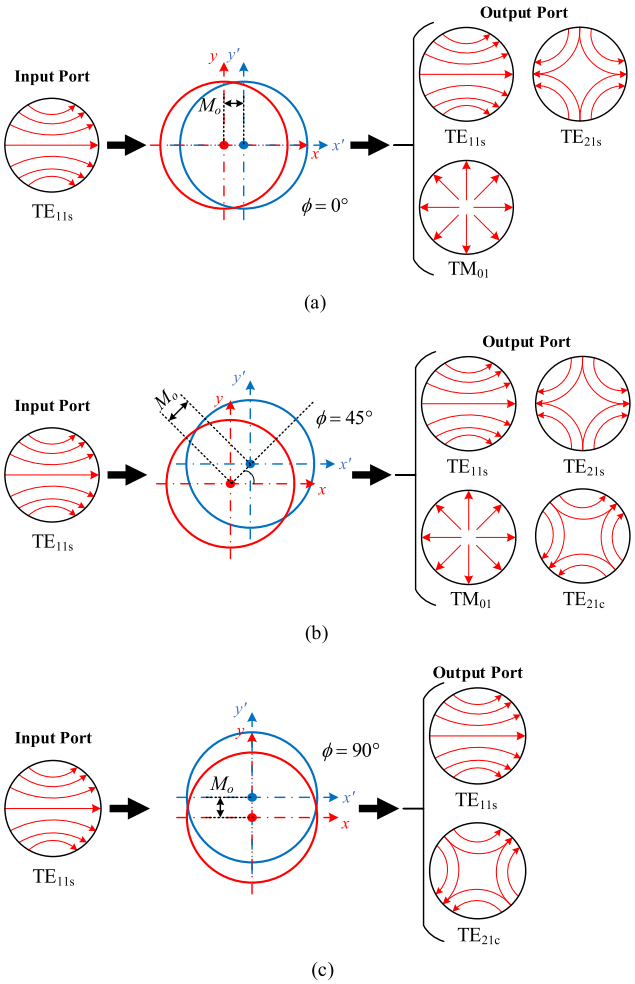

FIGURE 3. Generation of higher-order modes in the waveguide circuit with input horizontal polarization and different offset angles: (a) $\varphi = 0°$, (b) $\varphi = 45°$, (c) $\varphi = 90°$.

and elevation errors and working with a circular polarization can be designed only for mode TM_{01}, which leads to more simple feed systems [3], [17], [18]. If the tracking receiver was designed to manage both modes TE_{21} then a more flexible feed system would be obtained, since it would be able to work with both linear and circular polarizations with the throwback of a more complex structure.

B. SIGNAL SOURCE IMPLEMENTATION

The scheme described in Section II-A can be easily implemented in common commercial simulation tools based on linear models and techniques (S-Parameters) such as AWR Microwave Office from Cadence as shown in Fig. 4.

The first element, Port 1, is the input port of Fig. 1, which is configured through parameter PIN_DBM corresponding to the desired input signal power in dBm. For analysis purposes, it is convenient to set PIN_DBM = 0 dBm.

The second element is the net called GENERATOR. This subcircuit corresponds to the polarization generator in Fig. 1 and, consequently, its internal configuration has to be modified based on the desired signal polarization: for

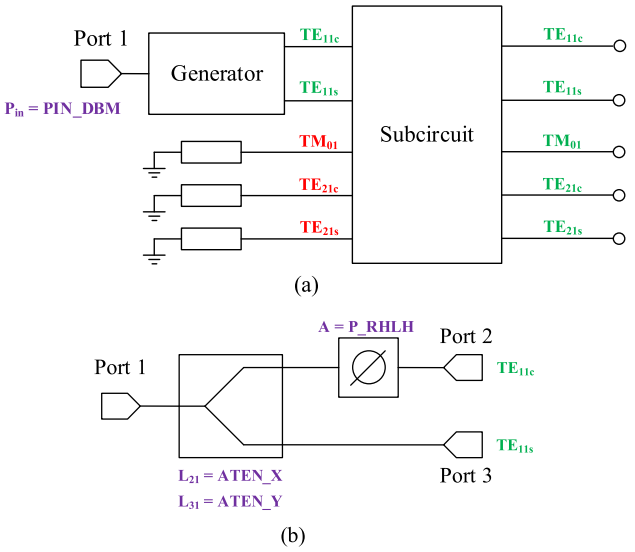

FIGURE 4. (a) Circuit schematic of the signal source implemented in AWR Microwave Office. The subcircuit GENERATOR can be configured to generate different polarizations; (b) detail of subcircuit GENERATOR able to produce a linear or a circular polarization.

linear polarization, the diagram presented in Fig. 4b should be used with the following parameters: ATEN_X and ATEN_Y are equal to the values obtained from (1) and (2) in dB respectively, and P_RHLH should be set to zero. For circular polarization, the single parameter P_RHLH configures the direction of rotation, ϕ, therefore, P_RHLH = 90° or −90° for LHCP or RHCP respectively, whereas parameters ATEN_X and ATEN_Y should be set to 3 dB.

Finally, the last element SUBCKT (in Fig. 4a) is the subcircuit containing the S-parameter file obtained from the FEM analysis of the HOMs generator. As explained in Section II, the nine simulations needed to obtain the corresponding S-parameters files, are introduced in this element sequentially or, preferably in parallel using nine different circuit schematics. In this way, the tracking contour can be obtained from a single circuital simulation run. In this work, the S-parameter files were obtained using the EM tool μWave Wizard from Mician. This tool is based on mode-matching techniques and provides very fast and accurate results for simple circuits like the HOM generator. Since five modes are considered in these simulations (from TE_{11} to TE_{21}), the HOMs generator dimensions need to be conveniently designed to enable the propagation of all these modes within the desired frequency range. Due to the symmetry and reciprocity of this circuit, a 10 × 10 S-parameter matrix is obtained from each simulation (five input modes and five output modes). Therefore, the three input modes that are not used at the input ports (TM_{01}, TE^s_{21} and TE^c_{21}) are closed on matched loads, as shown in Fig. 4a.

The five output ports of the signal source in Fig. 4a are fundamental and HOMs generated by the input signal with the desired power and polarization. These five signals are the input of an hypothetical tracking receiver

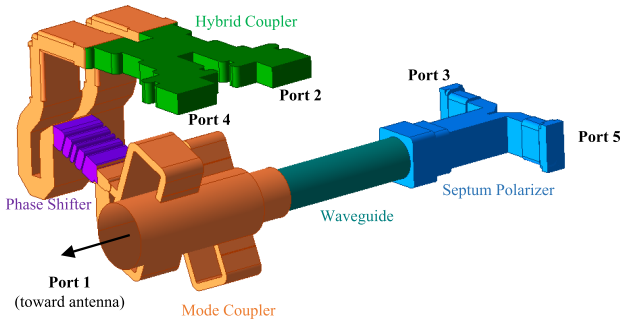

FIGURE 5. Antenna feed system with tracking capabilities designed to be analyzed with the proposed signal source.

extracting the data information from the fundamental modes and the azimuth-elevation information to pilot the antenna's servo-motor. The presented signal source and the workflow followed in this Section represent a clear advantage over other techniques [9] when simulating complex antenna feed systems with tracking capabilities.

III. ANTENNA FEED SYSTEM DESCRIPTION

In order to explain the workflow described in Section II and the capability to analyze an entire tracking system under different configurations, a complete circuit has been designed (see Fig. 5). To make more general this approach, the system does not include the antenna because its presence is not relevant for the analysis, since HOMs can be directly excited at the input port (Port 1). However, if desired, any antenna could be easily included.

The entire system is designed to work in X-band (8 – 8.5 GHz) using μWave Wizard and checked with CST Studio Suite and Ansys HFSS afterwards: it includes a resonant-type TE_{21} monopulse tracking coupler, similar to those in [6], [14], and [15], with standard WR112 rectangular tracking ports (Port2 and Port4 in Fig. 5) to extract the excited modes, and circular ports with radii $r_{in} = 19.9$ mm (Port1 in Fig. 5) and $r_{out} = 12.5$ mm (circular waveguide connecting to the septum polarizer). Tracking ports are connected to a Riblet-type hybrid coupler [19], [20] to perform the quadrature sum of the degenerate TE_{21} tracking signals. Moreover, this element physically separates both output ports so standard WR112 flanges can be connected to Ports 2 and 4. Between the tracking coupler and the hybrid coupler, a phase shifter is included in one branch to compensate the physical separation between the TE_{21s} and TE_{21c} coupling slots. Finally, as the feed system is intended to work with circular polarizations, a septum polarizer [21], [22], [23] is used to select one of the two circular orthogonal polarizations from the fundamental mode.

According to the configuration in Fig. 5, RHCP is at Port 5 and LHCP is at Port 3.

Fig. 6 presents some of the main performance results of the whole feed obtained from CST Studio Suite FEM simulations. Fig. 6a shows the axial ratio (AR) for the

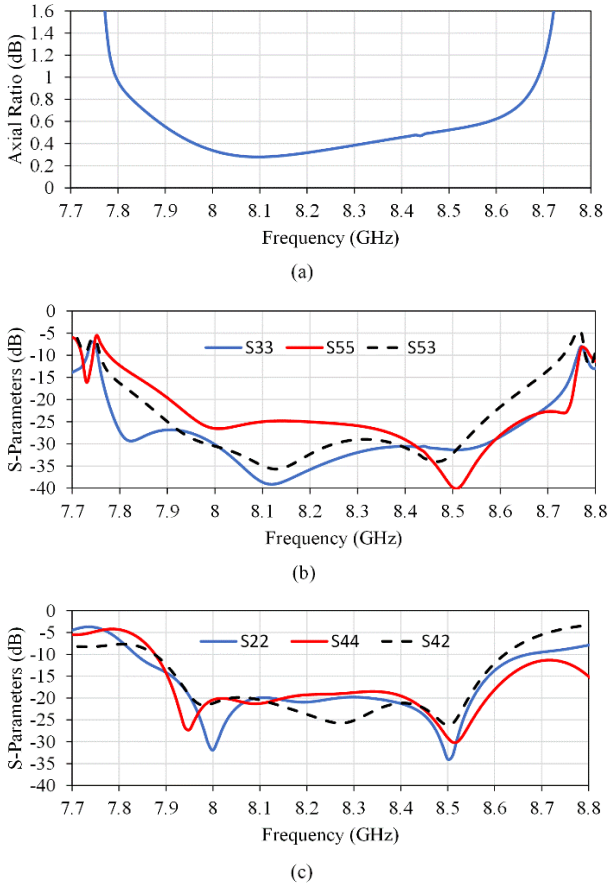

FIGURE 6. Simulated S-parameter results of the antenna feed system: (a) axial ratio for the fundamental mode; (b) matching and isolation at information ports: reflection at Port 3 (blue), reflection at Port 5 (red), isolation between Ports 3 and 5 (black dashed); (c) matching and isolation at tracking ports: reflection at Port 2 (blue), reflection at Port 4 (red), isolation between Ports 2 and 4 (black dashed).

fundamental mode (obtained at Ports 3 or 5) which is the parameter that defines the grade of polarization ellipticity, i.e. the goodness of the circular polarization for the fundamental mode. Typically, values of AR $\leq$ 1 dB, corresponding to a cross-polar discrimination greater than 25 dB, are considered as adequate in real applications; the value simulated is AR = 0.5 dB in the design band. Fig. 6b shows the simulated matching at information signal ports and the isolation between these ports with values better than -25 dB for the reflection and around 30 dB for the isolation. Finally, Fig. 6c presents the matching at tracking signal ports and transmission between these ports with values better than -18 dB for the reflection and around 20 dB for the isolation.

IV. DISCUSSION ON THE COMPUTATIONAL PROCEDURE AND EFFORT

The procedure followed to analyze the receiver configurations can be summarized as follows. First, the whole structure shown in Fig. 5 is analyzed by a full-wave tool and the scattering matrix is stored once for all, taking into account

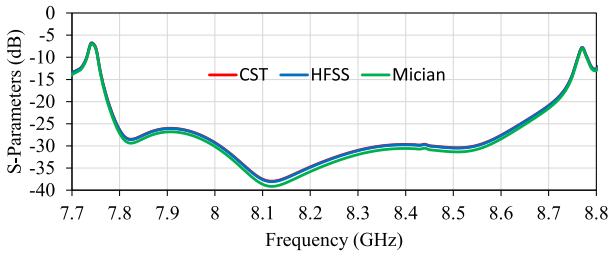

FIGURE 7. Reflection parameter at Port 3, comparison for different solvers: CST (red), HFSS (blue), Mician (green).

as many HOMs as required in the circular port. Then the scattering parameters of the HOM generator shown in Fig. 3 are calculated using μWave Wizard for many offsets M_0 and angle ϕ, thus mimicking different directions of arrival of the signal on the receiving antenna. Finally, the scattering matrices of the tracking system (schematic circuit in Fig. 8) and of the HOM generator (schematic circuit in Fig. 4) are cascaded by using Microwave Office. From the resulting scattering matrix, suitable plots are generated to show in a convenient way the depointing effect. It is noted that this last step is practically at no computation cost, regardless to the number of directions of arrival to be tested.

In order to give an insight on the computational effort, the simulation time and memory usage (both RAM for computation and hard disk for storage) are reported in Table 1. These results were obtained using a domestic hardware (Windows 10-x64, Intel Core i7-4790@3.60 GHz, Nvidia GeForce GT 730, 32 GB RAM). The full-wave analysis has been performed by CST Studio Suite (F-Solver [24], [25]), by Ansys HFSS with automatic adaptive meshing, and by μWave Wizard from Mician, which is based on the mode matching [26], [27]. Fig. 7 plots the matching at Port 3, showing a very good agreement between the different solvers.

V. DISCUSSION ON THE SIMULATED RESULTS WITH THE SIGNAL SOURCE

The proposed signal source shown in Fig. 4 is directly connected to the Port 1 presented in Fig. 5, in which the entire tracking system is characterized through an overall S-parameters file as shown in Fig. 8. Between these circuits, a power sampling element is connected in one of the HOM signal branches (TE_{21c}) in order to know the input power to the receiver. The subcircuit containing the feed S-parameters file has four outputs: the two information signals (TE_{11s} and TE_{11c}) and the two tracking signals (TE_{21s} and TE_{21c}). Between this subcircuit and the tracking output ports, ideal phase shifters are placed. The function of these phase shifters is to align the circuit response in phase with the depointing angle, thus for $\varphi = 0°$ the phase shifters values are set so the phase of the tracking signal exhibits the same value. The phase shifters values are obtained for this first angle simulation and are not modified for the other angles.

TABLE 1. Computational effort for the calculation of the scattering matrix of the tracking system (Fig. 5) for different solvers.

Software	Solver	Mesh elements	RAM (GB)	Storage (GB)	Time (min)
CST	FEM	335.327	5.2	11.3	90
HFSS	FEM	343.044	15.5	0.9	80
µWave Wizard	Mode Matching	N/A	2.0	0.01	45

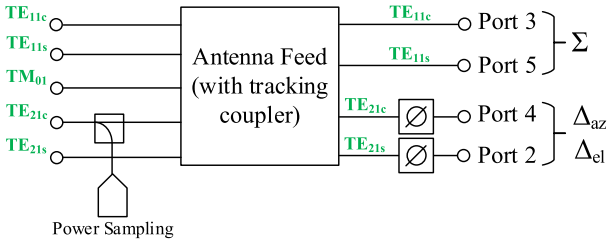

FIGURE 8. Circuit schematic for the simulation of the whole antenna feed system. This scheme is directly connected to the proposed signal source (Fig. 4).

A. CIRCULAR POLARIZATION WITH HYBRID COUPLER

The analysis starts with a RHCP and $P_{in} = 0$ dBm configured in the signal source (Fig. 4b). The magnitude of the waveguide offset in the HOM generator is $H_0 = 0.1$ mm which generates HOMs with a magnitude around 37 dB below the fundamental modes. This value is close to the null depth and representative of the real operation. The nine files of the HOMs generator with the nine angles defining the tracking contour (one at the boresight and eight offset angles) are loaded in the same number of circuit schematics so the responses are calculated and plotted in a single run. Results are presented in Fig. 9 in a polar plot so magnitude and angle values can be easily revised. Results are obtained at a single frequency within the design band, $f = 8.2$ GHz.

Figs. 9a and 9b present results at tracking ports. As can be seen in Fig. 9a, the tracking information is obtained at Port 2 with a total power of -37 dBm for angles $\varphi = 0°$ to $315°$ in $45°$ steps, which correspond to points A to H in Fig. 2b respectively, and enable to trace the tracking contour. Without any offset, i.e. at boresight, a power value of -110 dBm is obtained. This value is the theoretical (without horn) null depth of the DELTA radiation pattern for $\theta = 0°$. On its side, the other tracking port, Port 4, does not receive power. From Fig. 9b, a value of -70 dBm is read for all angles.

Regarding the information signals contained in the fundamental modes, since it is a RHCP signal, all the power is received at Port 5 (see Fig. 9c) whereas a value of -35 dBm leaks to Port 3 (see Fig. 9d).

This last value represents the isolation between information ports at the septum polarizer rectangular ports. In the case of a LHCP all the results are very similar to those presented in Fig. 9. The only remarkable differences are that the tracking ports and the information ports are exchanged,

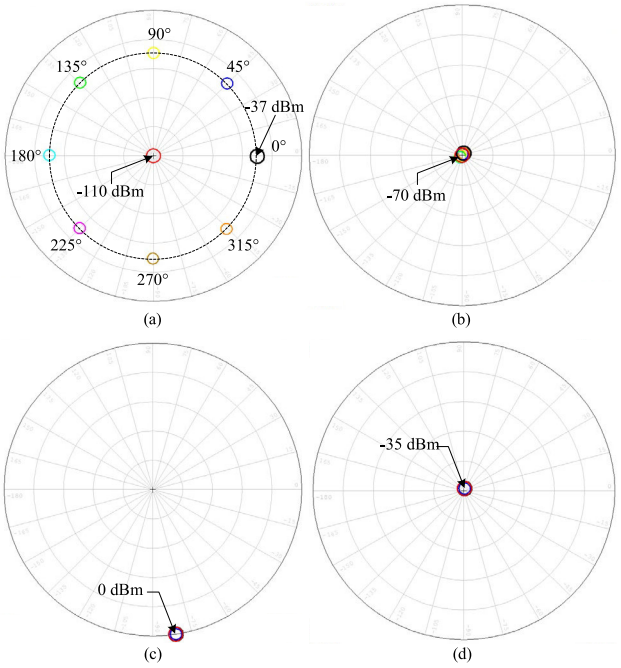

FIGURE 9. Simulated powers at different output ports for a RHCP input signal and different depointing angles φ: (a) tracking port 2; (b) tracking port 4; (c) information port 5; (d) information port 3.

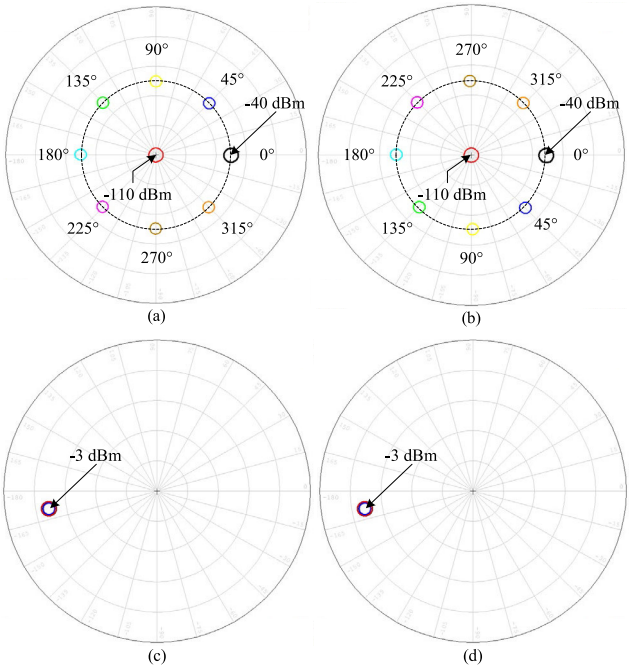

FIGURE 10. Simulated powers at different output ports for a linear input signal and different depointing angles φ: (a) tracking port 2; (b) tracking port 4; (c) information port 5; information port 3.

i.e. tracking information appears at Port 4 and information signal is at Port 3, and the rotation direction of the tracking contour is clockwise instead of counterclockwise. This last setback can be easily modified in the post processing stage just conjugating the tracking signal at the tracking receiver.

B. LINEAR POLARIZATION WITH HYBRID COUPLER

With the same parameters' values in the HOM generator and P_{in}, the input polarization is changed to linear so the corresponding signal source's parameters are configured in Fig. 4b. Results obtained in this case are plotted in Fig. 10 for all output ports. As can be checked in Figs. 10a and 10b, the same information is present at both tracking ports with conjugated results and a loss of 3 dB with respect to the circular polarization case. As a consequence, if an antenna feed system with a monopulse TE_{21} tracking coupler is used in a communication system working with linear polarization, then it is advisable not to use the hybrid coupler after the coupler. This case is analyzed in Section V-C. Regarding the information signal, due to the presence of a septum polarizer, half power is received in each port as can be seen in Figs. 10c and 10d. In this case, an orthomode transducer (OMT) would be preferable instead of the septum polarizer to carry out the orthogonal polarizations' separation function.

C. LINEAR POLARIZATION WITHOUT HYBRID COUPLER

To analyze the feed system without hybrid coupler, this element is removed from the circuit in Fig. 5 and simulated again. The resulting S-parameters is loaded in the corresponding subcircuit in Fig. 8. Now, the full system is simulated with a linear polarization input and the obtained results are presented in Fig. 11. As can be seen in Figs. 11a and 11b, the tracking information is divided between both ports: elevation error signal is sensed from Port 2, whereas azimuth error signal goes to Port 4. The combination of both tracking signals provides full information with a power level without any additional loss. The information signals, due to the septum polarizer, is evenly divided in this component and therefore, an additional loss of 3 dB is obtained at these ports, as plotted in Figs. 11 c and 11d.

D. CIRCULAR POLARIZATION WITHOUT PHASE EQUALIZATION

The last case in this analysis, introduced in Section III, is the configuration of the feed system where the phase shifter between the hybrid coupler and the tracking coupler is removed and the system works with a circular polarization. This configuration is intended to demonstrate the importance of the phase equalization in the tracking coupler. As in Section IV.C, the new feed configuration is simulated and the obtained S-parameters file is loaded in the circuit schematic of Fig. 8.

Fig. 12 shows the simulated results for this last configuration in which a RHCP signal has been introduced. Results are, in general, similar to those obtained with the phase shifter included, as can be checked comparing Figs. 9 and 12, but an important difference is observed in Fig. 12b. Some of the tracking information leaks to Port 4 and, consequently,

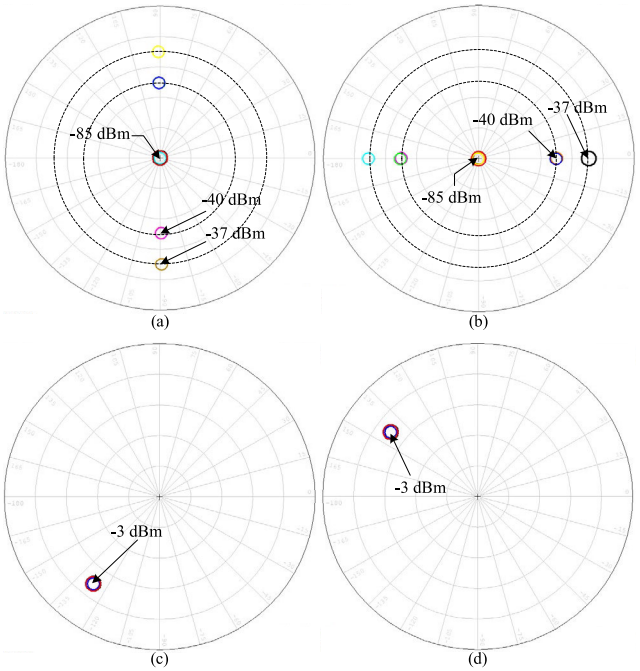

FIGURE 11. Simulated powers at different output ports for a linear input signal and different depointing angles φ in a feed system without hybrid coupler: (a) tracking port 2; (b) tracking port 4; (c) information port 5; information port 3.

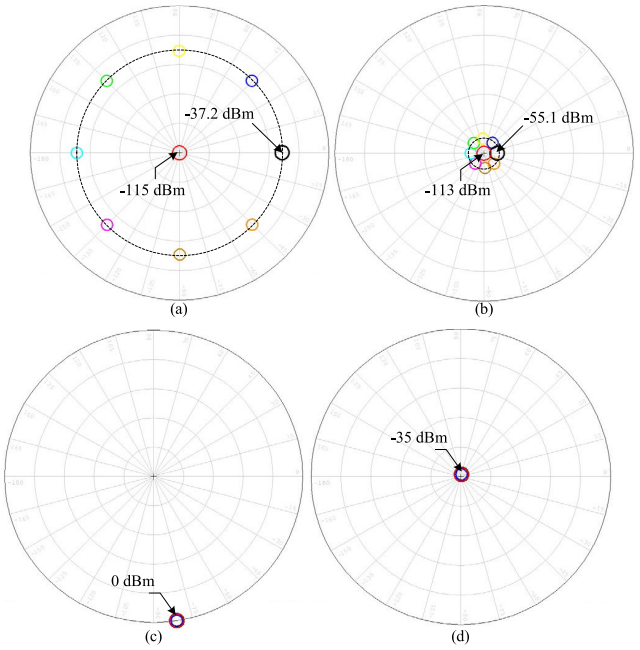

FIGURE 12. Simulated powers at different output ports for a circular input signal and different depointing angles φ in a feed system without phase shifter: (a) tracking port 2; (b) tracking port 4; (c) information port 5; information port 3.

the isolation between tracking ports is reduced from 33 dB to around 18 dB. This demonstrates the necessity of including the phase shifter to perform the phase compensation function and thus to improve the isolation between tracking ports.

VI. CONCLUSION

In this work, a simple schematic circuit that enables to implement an input signal source with defined power, polarization and controlled higher-order modes has been presented. This signal source is especially suitable for the simulation and analysis of complex antenna feed systems with multimode monopulse tracking capabilities through the emulation of real operation. The proposed simulation scheme is based on cascading the S-parameter matrices of the building blocks by a circuital technique, which reduce the simulation time and computational effort, unlike full-wave 3D EM simulations. This has been demonstrated with the analysis of the stand-alone tracking network without considering the antenna feed and the entire point-to-point tracking system.

The proposed signal source and simulation scheme can be directly adapted to any feed configuration including different types of multimode monopulse tracking couplers such as TM_{01} or TE_{01}.

It has to be pointed out that the examples reported in this paper do not fully consider the real-life scenario. In fact, the HOMs excitation depends not only on the direction of arrival of the signal, but also on antenna inaccuracies, such as the radiation pattern asymmetries, which are not considered. However, if the real HOMs excitation can be provided, the tool is able to calculate the correct tracking system performance. This demonstrates its great flexibility as a general simulation procedure.

ACKNOWLEDGMENT

The authors would like to acknowledge and thank Prof. Angel Mediavilla for his guidance, vast knowledge sharing, sound technical advice and, overall, for being a close and friendly fellow. His ideas and developments are in the basis of this work. Prof. Mediavilla passed away, in October 2022.

REFERENCES

[1] G. Hawkins, D. J. Edwards, and J. P. McGeehan, "Tracking systems for satellite communications," *IEE Proc., Part F*, vol. 135, no. 5, p. 393, Jan. 1988.

[2] S. M. Sherman and D. K. Barton, *Monopulse Principles and Techniques*, 2nd ed., Norwood, MA, USA: Artech House, 2011, ch. 1, pp. 13–15.

[3] Y. H. Choung, "Wideband TM_{01}-mode travelling wave coupler," *IEE Proc. Microw., Antennas Propag.*, vol. 144, no. 5, pp. 315–320, Oct. 1997.

[4] A. Tribak, A. Mediavilla, K. Cepero, and J. L. C. D. Diego, "Highly efficient monopulse tracking feed subsystem for unmanned aerial vehicle," in *Proc. 41st Eur. Microw. Conf.*, Manchester, U.K., Dec. 2011, pp. 1027–1030.

[5] Y. H. Choung, K. R. Goudey, and L. G. Bryans, "Theory and design of a Ku-band TE_{21}-mode coupler," *IEEE Trans. Microw. Theory Techn.*, vol. MTT-30, no. 11, pp. 1862–1866, Nov. 1982.

[6] S. M. M. Azizi and S. H. Mohseni Armaki, "A compact TE_{21} mode coupler for tracking purposes," *IEEE Microw. Wireless Compon. Lett.*, vol. 28, no. 6, pp. 470–472, Jun. 2018.

[7] E. Schuegraf, "Tracking system for satellite ground station antennas with field-selective coupling of TE_{01} and TM01 modes," in *Proc. 20th Eur. Microw. Conf.*, Budapest, Hungary, Oct. 1990, pp. 1589–1593.

[8] T.-H. Chang and C.-F. Yu, "High order mode electromagnetic wave coupler and coupling method using proportional distributing waves," U.S. Patent 7 369 011 B2, May 6, 2008.
[9] K. Kwon, J. Park, W. Kim, H. Lee, D. Park, and J. Heo, "Design X-band monopulse tracking system," *Microw. Opt. Technol. Lett.*, vol. 61, no. 8, pp. 2027–2032, Mar. 2019.
[10] G. Ceccato, J. L. C. D. Diego, A. Mediavilla, and L. Perregrini, "Controlled high order mode generation for tracking coupler bench test," in *IEEE MTT-S Int. Microw. Symp. Dig.*, Los Angeles, CA, USA, Aug. 2020, pp. 904–907.
[11] G. Ceccato, J. L. Cano, A. Mediavilla, and L. Perregrini, "Controlled excitation of waveguide high-order modes for a simple and accurate monopulse tracking system test bench," *IEEE Trans. Microw. Theory Techn.*, vol. 69, no. 2, pp. 1327–1334, Feb. 2021.
[12] G. Ceccato, J. L. Cano, A. Mediavilla, and L. Perregrini, "A simple and accurate method for circularly polarised monopulse TM01 tracking system testing," in *Proc. 23rd Int. Microw. Radar Week (MIKON)*, Varsovia, Polonia, Oct. 2020, pp. 218–221.
[13] S. J. Hamada and T. Yodokawa, "Multi-mode tracking antenna feed system," U.S. Patent 4 420 756, Dec. 13, 1983.
[14] A. K. Pandey, "Design of multimode tracking system for Earth station antenna," in *Proc. Asia–Pacific Microw. Conf. (APMC)*, New Delhi, India, Dec. 2016, pp. 1–4.
[15] C. Barquinero, J. Gómez, A. Mediavilla, J. L. Besada, and B. Galocha, "A compact simultaneous K/S monopulse tracking feed for future Earth observation applications," in *Proc. 15th Eur. Radar Conf. (EuRAD)*, Madrid, Spain, 2018, pp. 349–352.
[16] Y.-J. Lee, W.-L. Chen, S.-K. Yaung, R.-M. Yang, M. Chen, C.-Y. Chu, and S. Chung, "Design of antenna feed for mono-pulse auto-tracking ground station," in *Proc. Asia–Pacific Microw. Conf. (APMC)*, Sendai, Japan, Nov. 2014, pp. 301–303.
[17] H. Bayer, A. Krauss, R. Stephan, and M. A. Hein, "Multimode monopulse tracking feed with dual-band potential for land-mobile satellite communications in Ka-band," in *Proc. 5th Eur. Conf. Antennas Propag. (EUCAP)*, Rome, Italy, Apr. 2011, pp. 1169–1172.
[18] N. J. G. Fonseca, "Very compact TM01 mode extractor for enhanced RF sensing in broadband satellite multiple beam reflector antenna systems," in *Proc. 8th Eur. Conf. Antennas Propag. (EuCAP)*, The Hague, Netherlands, Apr. 2014, pp. 260–264.
[19] H. Riblet, "The short-slot hybrid junction," *Proc. IRE*, vol. 40, no. 2, pp. 180–184, Feb. 1952.
[20] L. T. Hildebrand, "Results for a simple compact narrow-wall directional coupler," *IEEE Microw. Guided Wave Lett.*, vol. 10, no. 6, pp. 231–232, Jun. 2000.
[21] F. Dubrovka, S. Piltyay, O. Sushko, R. R. Dubrovka, M. M. Lytvyn, and S. M. Lytvyn, "Compact X-band stepped-thickness septum polarizer," in *Proc. IEEE Ukrainian Microw. Week (UkrMW)*, Kharkiv, Ukraine, Sep. 2020, pp. 135–138.
[22] Z. Ding, R. Jin, S. Yang, and X. Zhu, "Design of septum polarizer waveguide feed manufactured by split-block technique," in *Proc. IEEE Int. Symp. Antennas Propag. North Amer. Radio Sci. Meeting*, Montreal, QC, Canada, Jul. 2020, pp. 1939–1940.
[23] W. Zhong, B. Li, Q. Fan, and Z. Shen, "X-band compact septum polarizer design," in *Proc. IEEE Int. Conf. Microw. Technol. Comput. Electromagn.*, Beijing, China, May 2011, pp. 167–170.
[24] W. K. Liu, S. Li, and H. S. Park, "Eighty years of the finite element method: Birth, evolution, and future," *Arch. Comput. Methods Eng.*, vol. 29, no. 6, pp. 4431–4453, Jun. 2022.
[25] S. Piltyay, A. Bulashenko, Y. Herhil, and O. Bulashenko, "FDTD and FEM simulation of microwave waveguide polarizers," in *Proc. IEEE 2nd Int. Conf. Adv. Trends Inf. Theory (ATIT)*, Kyiv, Ukraine, Nov. 2020, pp. 357–363.
[26] J. M. Reiter and F. Arndt, "Rigorous analysis of arbitrarily shaped H- and E-plane discontinuities in rectangular waveguides by a full-wave boundary contour mode-matching method," *IEEE Trans. Microw. Theory Techn.*, vol. 43, no. 4, pp. 796–801, Apr. 1995.
[27] F. Arndt, R. Beyer, J. M. Reiter, T. Sieverding, and T. Wolf, "Automated design of waveguide components using hybrid mode-matching/numerical EM building-blocks in optimization-oriented CAD frameworks-state of the art and recent advances," *IEEE Trans. Microw. Theory Techn.*, vol. 45, no. 5, pp. 747–760, May 1997.

JUAN LUIS CANO was born in Torrelavega, Spain, in 1979. He received the Ingeniero de Telecomunicación and Ph.D. degrees from Universidad de Cantabria, Santander, Spain, in 2004 and 2010, respectively.

He is currently a Researcher with Universidad de Cantabria, Spain, where he collaborates in the development and measurement of microwave receivers for radio astronomy and satellite applications. His research interests include the design and testing of low-noise amplifiers (LNA) in MIC and MMIC technologies both at room and cryogenic temperatures, the design of different hardware for antenna feed networks, and the development of new technologies for efficient subsystems in multi-pixel microwave cameras.

GABRIELE CECCATO (Member, IEEE) was born in Novi Ligure, Italy, in 1993. He received the M.S. degree in electronic engineering from the University of Pavia, Italy, in 2017, and the dual Ph.D. degree in electronic and computer science from the University of Pavia and the University of Santander, Spain, in 2022. He is currently pursuing the M.S. degree in biomedical engineering with the University of Genoa. In 2021, he joined RINA Consulting S.p.A., where is an Electromagnetic Engineer. His research interests include the design of microwave components for space communications and wearable sensors for sports activities.

LUCA PERREGRINI (Fellow, IEEE) was born in Sondrio, Italy, in 1964.

He is a Full Professor of electromagnetic fields with the University of Pavia, where he is currently the Dean of the Faculty of Engineering and responsible of the Microwave Laboratory. He was a Visiting Professor with École Polytechnique de Montréal, Canada, from 2001 to 2006. He has been responsible for many research contracts with prominent international research centers and companies. He has authored more than 120 journal articles, more than 300 conference papers, six book chapters, and two textbooks, and co-edited the book *Periodic Structures*. He received several best paper prizes at international conferences. His main research interests include numerical methods for electromagnetic structures, microwave passive circuits, quasi-optical frequency multipliers, frequency-selective surfaces and metasurfaces, and antennas.

Prof. Perregrini has been a member of the Board of Directors of the European Microwave Association (EuMA), from 2016 to 2024, the EuMA General Assembly, from 2011 to 2013, prize committees for several conferences/societies, and the Technical Committee MTT-1 (Microwave Field Theory) of the IEEE Microwave Theory and Technique Society (MTT-S). He was a co-recipient of several best paper awards at international conferences. He was the Chair of the Fellow Evaluation Committee of MTT-S, from 2023 to 2024. He served as the General Chair of the European Microwave Week 2022, the TPC Chair of the IEEE MTT-S NEMO 2014, the TPC Chair of EuMC 2014, and the TPC Chair of IWS-AMP 2017. He has been the Editor-in-Chief of IEEE Transactions on Microwave Theory and Techniques, from 2017 to 2019, and an Associate Editor of IEEE Microwave and Wireless Components Letters, from 2010 to 2013, IEEE Transactions on Microwave Theory and Techniques, from 2013 to 2016, IJMWT, from 2011 to 2016, and *Electronic Letters* (IET), from 2015 to 2016. He was an invited speaker at several conferences, universities, and research centers worldwide.